Mine Water and the Environment (2021) 40:74–82
https://doi.org/10.1007/s10230-021-00753-7

TECHNICAL ARTICLE

Pyrite Flotation Separation and Encapsulation: A Synchronized Remediation System for Tailings Dams

P. Camero-Hermoza[1] · D. Calla-Choque[2] · J. C. Rojas-Montes[3] · C. Villachica-Leon[4] · J. Villachica-Llamosas[4]

Received: 3 February 2020 / Accepted: 14 January 2021 / Published online: 28 January 2021

Abstract
Pyrite flotation separation and encapsulation in tailings dams is proposed as a viable way to chemically stabilize tailings. Characterization of potential acid mine generation in tailings led to an innovative process in which acid-generating pyrite is separated by flotation from the coarse tailings and incorporated into the slime zone. This creates pyrite-free neutral tailings acceptable for placement in the dyke and permanently avoids acid generation.

Keywords Acid mine drainage · Pyrite encapsulation · Acid potential · Slimes

Introduction

Proper tailings management can help prevent environmental problems with tailings ponds (Gabarrón et al. 2019). When the deposit contains pyrite, there is a risk of acid generation and the dissolution of other metal sulfides in the tailings (Olías et al. 2016; Wang et al. 2017). The potential generation of acid mine drainage (AMD) can be predicted by static and dynamic geochemical tests (Fairgray et al. 2019). Static tests consider the balance between minerals that can produce acidity and those that neutralize; acid drainage occurs when the acid generation capacity (acid potential, AP) of the tailings exceeds their neutralization capacity (neutralization potential, NP). AP can be modified by separating the pyrite, which is usually the predominant sulfide. The NP depends on carbonates, oxides, and silicates of different neutralization capacity and the net neutralization potential (NNP) results from the relationship of the AP and NP values (NNP = NP − AP). Therefore, AMD can be avoided by separating the pyrite from the tailings. Alternatively, the water can be treated using active and passive methods (e.g. Calla-Choque 2012; Younger et al. 2002; Santos Jallath et al. 2018).

Characterizations carried out on Peruvian tailings dams have determined that embankment dykes built with cyclone underflow tailings produce acid drainage zones, as the pyrite is concentrated due to its density (5.4 g/mL) being higher than the rest of the tailings minerals (2.7 g/mL). On the other hand, the hydrocyclone overflow, conformed by slimes, has a limited pyrite content and a higher NP than the original tailings. Pyrite in the highly permeable dyke is rapidly oxidized. In contrast, the very low permeability in the zone of fines and slimes prevents air access and significantly limits pyrite oxidation.

Pyrite flotation is a well-known and inexpensive method (Moslemi and Gharabaghi 2017; Santander and Valderrama 2019; Wang and Forssberg 1991) because flotation chemicals and process water can be almost completely recycled due to the coarse particle size of the hydrocyclone underflow. In Peru, four companies have programmed this system into the final stage of closing their tailings deposits.

With this in mind, a system (Fig. 1) was developed for pyrite encapsulation at a site where two concentrates (Cu–Pb and Zn) are obtained from the ore deposit. The tailings go to the hydrocyclone, where the pyrite in the underflow is separated by flotation or gravimetry. The concentrate thus obtained (called "acid tailings") is submerged in the slime

✉ D. Calla-Choque
dcalla@outlook.com

1 Academic Department of Metallurgical Engineering, National University of San Antonio Abad del Cusco (UNSAAC), Av. La Cultura 773, CP 08000 Cusco, Peru

2 Faculty of Engineering, National Autonomous University of Mexico (UNAM), 04510 Mexico City, Mexico

3 Cátedras CONACyT-TecNM/I.T. Durango, Felipe Pescador 1830 Ote. Col. Nueva Vizcaya, Durango, C.P. 34080 Dgo, Mexico

4 Consulcont S.A.C, Research Center, Dario Valdizan 237, Engineering Urbanization, Lima 31, Lima, Peru

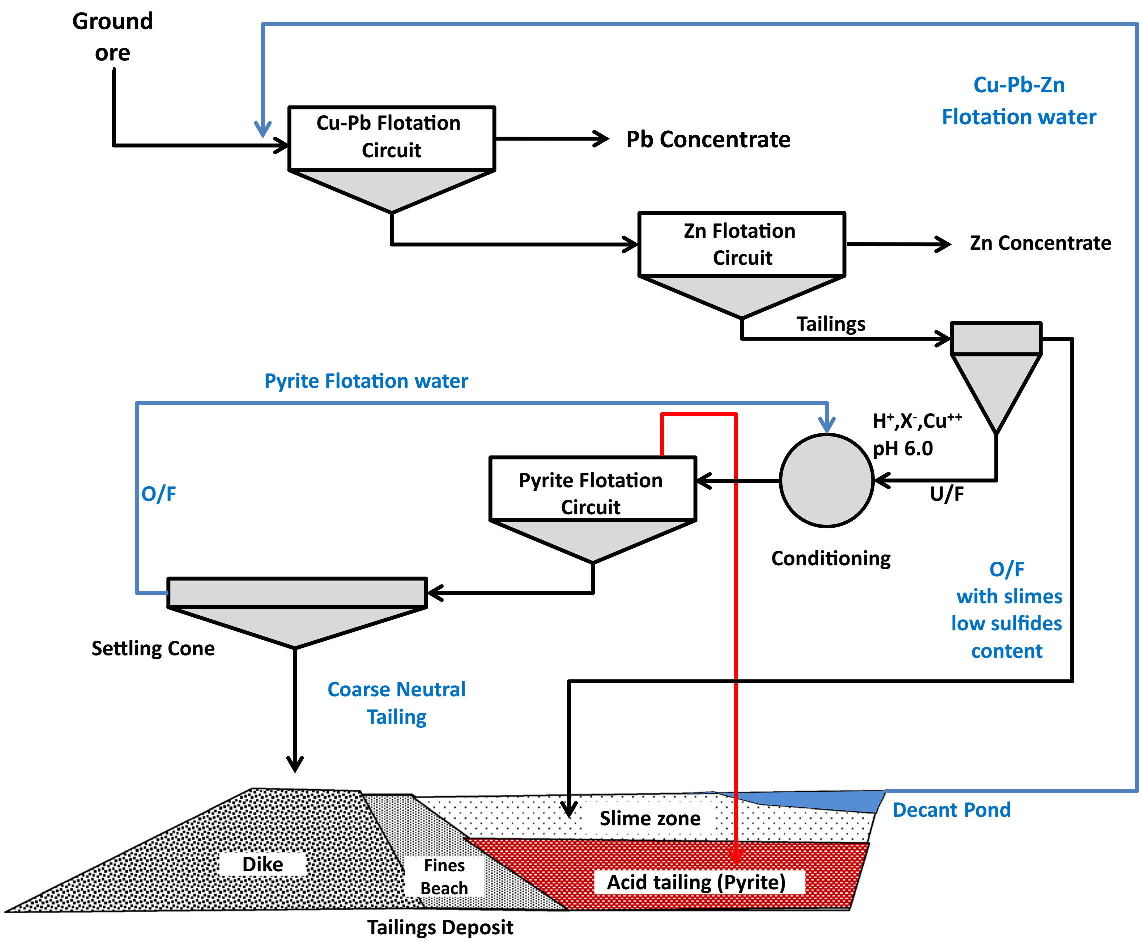

Fig. 1 Schematic diagram of pyrite encapsulation system in tailings dam

zone to prevent oxidation. The pyrite flotation tailings (called "neutral tailings") are easily dewatered and placed in the dyke. Due to its higher density relative to the fine material, the pyrite in the tailings dam sinks down and is isolated from the air. In this manner, AMD generation can be permanently avoided.

Site Description

The production unit, located in the Central Sierra of Peru, 120 km east of the city of Lima and 14 km east of the city of San Mateo, in Huarochiri Province and the Department of Lima-Peru (Fig. 2), has an average monthly rainfall of 176.02 mm with summer high temperatures of 18–20 °C and winter temperatures of 5–17 °C. It is classified as a tundra climate using the ET Köppen-Geiger classification method (Kottek et al. 2006; Mazzeo et al. 2020).

In this processing unit, two concentrates are obtained, Cu–Pb and Zn, the produced tailings have a mineralogical composition of 0.17% chalcopyrite, 0.29% galena, 0.39% sphalerite, and 14% pyrite determined by x-ray fluorescence analysis. The chemical composition was analyzed in an atomic absorption spectrometer (Table 1). From these tailings, the separation and encapsulation of pyrite were studied according to the scheme presented in Fig. 1, which begins in the cyclone stage followed by a pyrite flotation stage and evaluation of the products generated, according to their acid drainage potential.

Experimental Methods

Settling Speed

The sedimentation rate test conditions are shown in Table 2; tailings from two tailings dams, Chinchan and Arirahua, were used. The clean pyrite concentrate was obtained on a vibrating table from the underflow of the Chinchan tailings dam and classified in 100, 140, and 200 mesh (group one, two, and three, respectively). On the other hand, the overflow of the Arirahua tailings

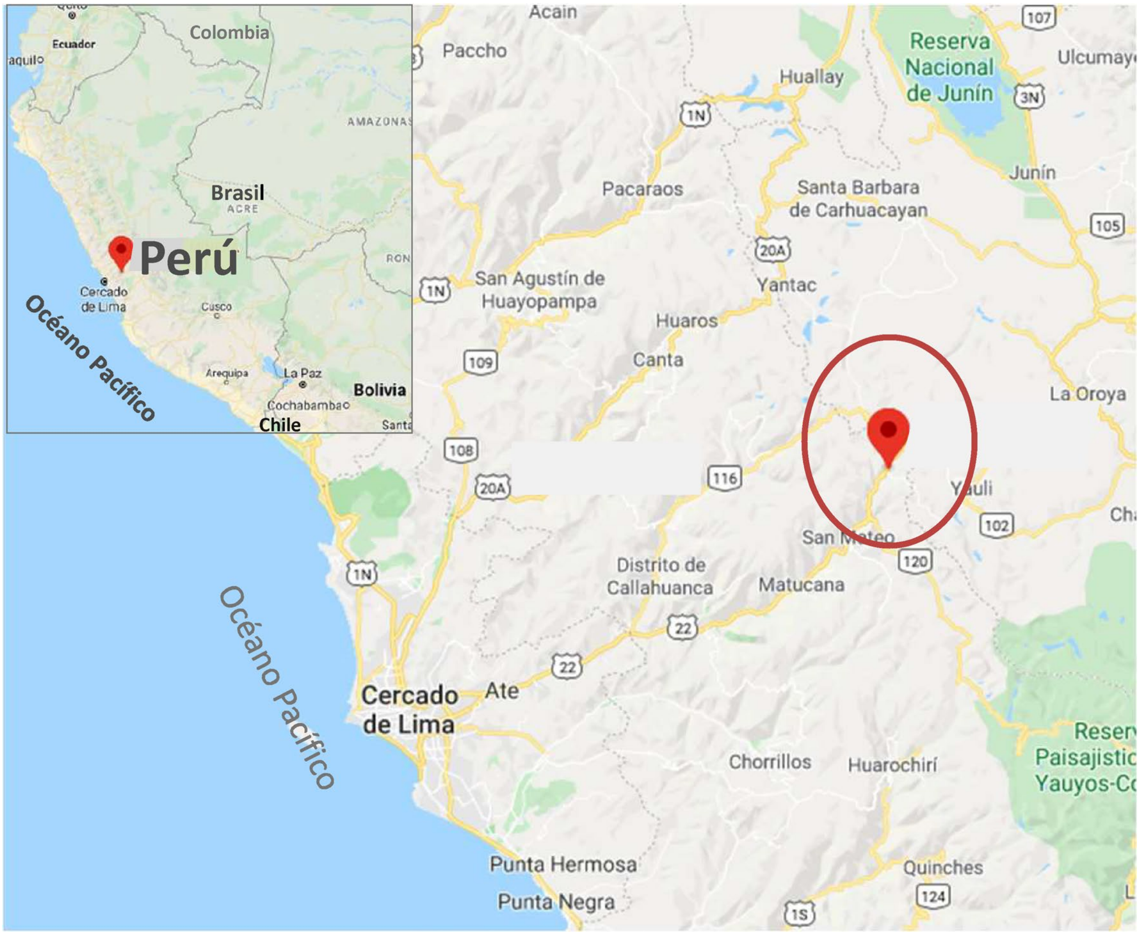

Fig. 2 Site description

Table 1 Chemical composition of the flotation tailings (%wt)

Cu	Pb	Zn	Fe	S	As	Sb	Mn	SiO_2
0.05	0.25	0.26	7.6	9	0.06	0.02	0.31	50.9

Table 2 Settling conditions

Time	1 min			2 min		
Mesh	100	140	200	100	140	200
Layer	1	1	1	1	1	1
	2	2	2	2	2	2
	3	3	3	3	3	3
	4	4	4	4	4	4
	5	5	5	5	5	5

dam of 200 mesh was used for the fines. Both products were mixed in a 1000 mL flask, stirred for 10 min and allowed to settle for 1 and 2 min; one sample per layer was siphoned off, which was weighed, sieved, filtered, and dried to determine the pulp weight, solids weight, solids concentration, and pyrite distribution in each layer. These tests are semi-quantitative because the pyrite concentration in the different layers was quantified assuming that the pyrite concentrate is pure; a complete chemical analysis was not performed because these were exploratory tests.

Underflow Pyrite Flotation

For the flotation tests, the material originating from the cyclone underflow at the Chinchan tailings dam were tested in a Denver Sub-A flotation cell at 1500 rpm, with 0.050 kg/t of sodium isopropyl xanthate (Z-11) as the collector and 0.1 kg/t of D-1012 as the frothing agent. The samples were repulped to 38% solids. The conditions are summarized in Table 3.

The objective of these tests was to achieve the greatest separation, with the pyrite in the underflow to be stored under water, in the fines bed (with the low-sulfur tailings having little or no acid-generating capacity). The weight ratio of concentrate to tailings, the sulfur content in the products, and its neutralization capacity were all evaluated. For the underflow flotation products, chemical characterization of the tailings was evaluated by the float time, with quantification of S and $CaCO_3$ in each stage (Table 2), to calculate acid potential (AP), neutralization potential (NP), and net potential (NNP) for each flotation stage.

Encapsulation Tests Pyrite Concentrate

To evaluate the behavior of a sample and simulate the encapsulation of the pyrite concentrate obtained by flotation from the underflow, five sedimentation tests were developed, maintaining the quantities of the pyrite and fine concentrates constant; agitation time, total volume, and sedimentation were evaluated (Table 4). All tests were conducted with a stirring time of 10 min. Sedimentation after 5, 10, 15, 20, and 30 min were measured in a 1000 mL graduated cylinder with a manual vertical axis agitator with a perforated disk. After the sedimentation time was completed, 200 mL of each of the five layers was siphoned off, weighed, filtered, dried, and analyzed for sulfur and calcium carbonate to determine the NNP of each layer.

Table 4 Encapsulation tests conditions with 204.5 g pyrite, 278.1 g fine concentrates for different sedimentation times

Pulp (mL)	Time (min)	
	Stirring	Sedimentation
1000	10	5
		10
		15
		20
		30

Granulometric and Chemical Characterization

The granulometric characterization of the feed to the cyclone (plant tailings), the underflow, overflow, pyrite concentrate, and the neutral tailings (underflow flotation tailings) were performed by mesh analysis (ASTM D4513-11 2017). As previously mentioned, chemical characterization allows determination of the AP, NP, and NNP values. Sulfur was determined gravimetrically based on the transformation of all sulfur forms into sulfate ions in a hydrochloric acid (HCl) solution followed by the addition of barium chloride ($BaCl_2$) and the precipitation of barium sulfate ($BaSO_4$). The precipitation was carried out near the boiling temperature, and after a period of digestion, the precipitate was filtered, washed with water until free of Cl^-, calcined or dried, and weighed as $BaSO_4$. The $CaCO_3$ was determined by titration in accordance with Standard Methods 2320 B (Clesceri et al. 1999).

Results and Discussion

Settling Speed

The settling test results show the influence of particle size on pyrite's sedimentation rate within a pulp (Fig. 3a–c, group one two, and three, respectively). The percentage of pyrite retained in the upper layers (bars) for the first and second groups (Fig. 3a, b) was less than 1%. For both 1- and

Table 3 Underflow flotation test conditions

Test	Wet weight (g)	Water (mL)	Time (min)						
			Repulping (min)	conditioning I	Ro I	RoII	RoIII	conditioning II	Sc.
PY-1	600	730	5	5	1	1	1	4	5
PY-2	600	730	5	5	1	1	2	4	5
PY-3	600	730	5	2.5	2			2	3
PY-4	600	730	3	2	2			2	3
PY-5	3000	3700	3	5	3			2	3

Ro rougher flotation, *Sc* scavenger flotation

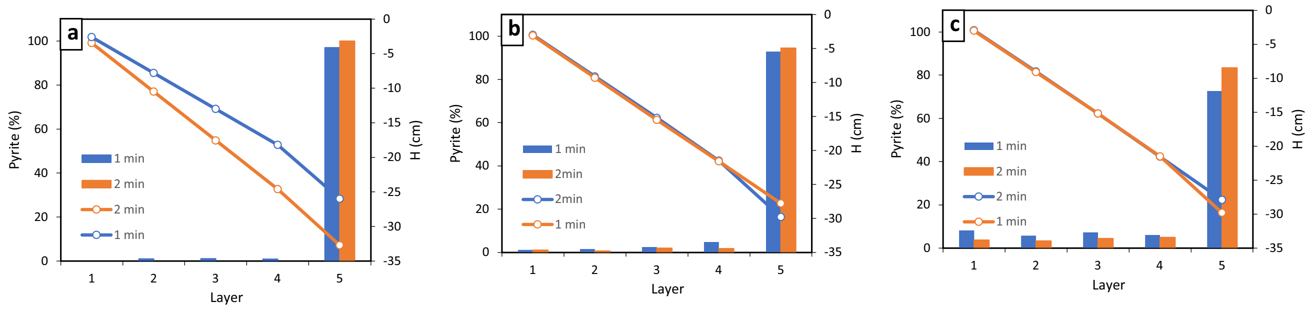

Fig. 3 Sedimentation rate (cm, lines) and % pyrite retained at different layers (%, bars) **a** mesh 100, **b** mesh 140 and **c** mesh 200

2-min settling times (lines), more than 94% of the pyrite was deposited in the bottom layer, while for the third group, only 72% of the pyrite was in the bottom layer after 1 min and 83% after 2 min. These results are consistent with previously published pyrite sedimentation rate studies (Vergouw et al. 1998). The percentage pyrite distribution in the different layers is mainly independent of mesh size, allowing the use of this process to encapsulate pyrite at the bottom of the tailings pond.

Pyrite Flotation

These tests were aimed at separating the pyrite contained in the cyclone underflow so that they can be stored underwater in the fines area. The flotation tails, which contains low-sulfur tailings with little or no acid-generating capacity are currently being used as filler material in the construction of the dyke. The pyrite inclusion in this material reduces the generation of the dam's AMD, controlling the weight ratio of concentrate to tailings, the sulfur content in the products and its neutralization capacity. Therefore, five tests were carried out to evaluate the degree of pyrite separation by the flotation process; acidity generation potential was determined by quantifying S and $CaCO_3$. For the flotation tests, the following stages were used: conditioning I, Rougher I, II and III for tests 1 and 2 (PY-1, PY-2, group I); and for tests 3, 4, and 5 (PY-3, P-Y4, PY-5, group II), the conditioning stages I, Rougher I, conditioning, and Scavenger were used, according to the conditions presented in Table 3.

From the results of tests 1 and 2 (group I), the AP of the concentrate decreases with flotation time (Fig. 4a); similar behavior was observed in tests 3, 4, and 5 (group II, Fig. 4d). The generation of AP in the tailings is constant in both groups and is directly related to the sulfur content, as was mentioned previously; in contrast, the NP increases in the concentrate (Fig. 4b, e), which may be explained by increased entrainment of carbonate components in the flotation process, while this remains essentially constant in the tailings.

Figure 4c, f shows that a highly water-generating concentrate with an NNP less than 700 kg of $CaCO_3$/t can be achieved through flotation. To avoid potential acidification, the NNP should exceed + 20 or + 30 kg $CaCO_3$/t (Lottermoser 2010); alternatively, the concentrate can be stored in ways to avoid or mitigate AMD generation, such as the underwater storage proposed in this work.

Most importantly, these flotation tests show that neutral or relatively neutral tailings are achievable with different flotation times. The NNP of the tailings take on a value of − 31.96 kg of $CaCO_3$/t with 1 min of flotation and up to + 36.43 kg of $CaCO_3$/t with 6 min of flotation. The higher NNP values provide greater security and environmental advantages, since the dyke would be covered by material with little or no capacity to generate AMD. In the closing stage of operations, this would entail lower tailings treatment costs and greater security regarding the chemical stability of a tailings dam.

Granulometric and Chemical Characterization

In accordance with the objectives of the present work, the feed to the cyclone (plant tailings), the underflow, overflow, pyrite concentrate and the neutral tailings (flotation tailings) were granulometrically characterized using a series of sieves (ASTM). The results of this analysis are shown in Table 5, where 85% of the pyrite concentrate > 400 mesh (Fig. 5); this granulometry will allow the sedimentation of the pyrite material, due to its density being greater than the other material in the fines area of the pond. The Chinchan dam pond is made up of nearly 100% < 400 mesh material, with a density much less than that of the concentrate; the particle size of the neutral tailings does not appreciably vary compared to the granulometry of the underflow, with an error less than 7% (Table 5). Therefore, the stability of the dyke will not be affected by this variable.

Chemical characterization of the components of each test allowed the AP, NP, and NNP values to be determined, as well as their variations during the sedimentation process (Table 6). These values show that the underflow, which is

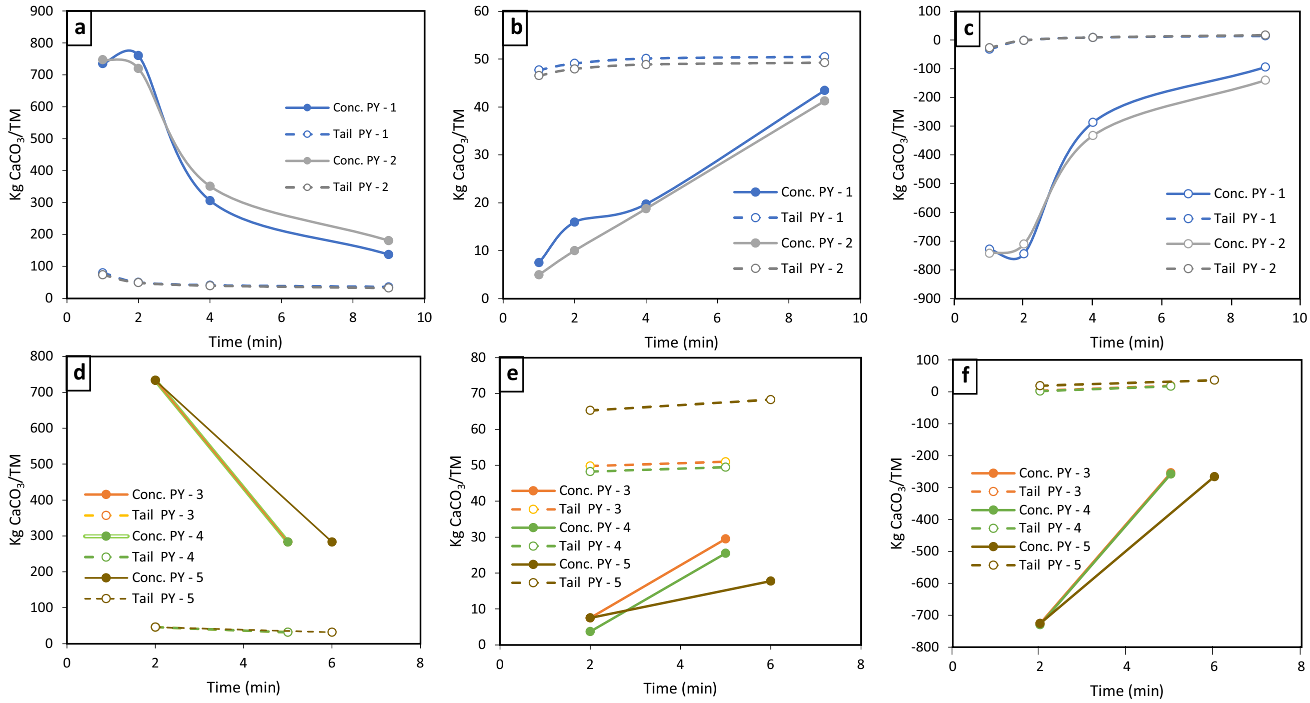

Fig. 4 Pyrite flotation time **a** acid potential (AP), **b** neutralization potential (NP), **c** net neutralization potential (NNP) for the tests PY-1 y PY-2 and **d** AP, **e** NP, **f** NNP for the tests PY-3, PY-4 y PY-5

Table 5 Granulometric characterization of sedimentation test components (near 500 g samples)

Mesh		Feed		Underflow		Overflow		Conc. FeS_2		Neutral Tail	
Num.	Diam (µm)	g	%	g	%	g	%	g	%	g	%
70	212	111.8	22.7	193.5	38.1	9.1	2.0	14.4	3.9	151.5	38.6
100	150	55.2	11.2	97.7	19.2	8.5	1.8	31.7	8.6	74.8	19.1
200	75	80.9	16.4	103.1	20.3	65.0	14.0	140.2	38.0	94.8	24.1
400	38	83.4	16.9	67.8	13.3	111.8	24.1	125.2	34.0	32.5	8.3
– 400	< 38	162.2	32.9	46.1	9.1	270.5	58.2	57.2	15.5	39.2	10.0
∑ Weight (g) Calc		493.6		508.2		464.9		368.7		392.8	
Error		6.4		1.8		5.1		3.3		6.2	

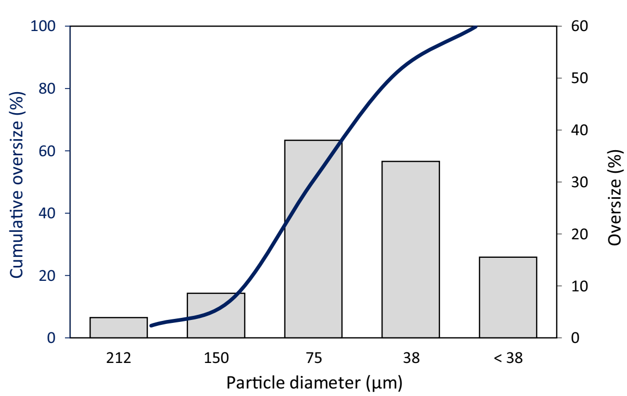

Fig. 5 Particle distribution of the pyrite concentrate

currently stored in the Chinchan dam, is a high-grade AMD generator. After implementing the flotation process, neutral tailings can be stored in the dyke. On the other hand, the pyrite concentrate (a high AMD generator), would be encapsulated below the fines, which have less capacity to generate AMD.

Comparing the results of the five tests allows the values of the variables to be studied as a function of settling time. Values obtained at the same depth (layer) for the different settling times are shown in Fig. 6. The % solids (% weight) in the pulp of the first layer (3.4 cm) decreased over time (Fig. 6a), while it remained almost constant in the second and third layers (10.2 and 17 cm), and tended to increase in the fourth and fifth layers (23.8 and 30.6 cm). The % sulfur in the bottom four layers was low and decreased slightly over time (Fig. 6b), while the fifth layer increased slightly over time. Consequently, a similar tendency was observed with the AP: low AP values for the upper layers and very high in the bottom layer (Fig. 6c). Meanwhile, examining the NP shows that this value was high in the upper layers, with a tendency to increase over time, and lower in the bottom layer, although with somewhat irregular behavior (Fig. 6d). Finally, the NNP values are negative in the upper layers with a clear tendency to increase over time and be even more negative in the bottom layers (Fig. 6e), with a projection to more negative values. There is a tendency for the NP/AP ratio (Fig. 6f) to increase over time in the upper layers, while approaching zero in the bottom layer; a value close to zero in the NP/AP denotes an acid-generating potential, while a value close to 1 indicates little to no acid-generating capacity.

The sulfur accumulation (%) increased with depth and decreased with settling time, while the exact opposite

Table 6 Chemical characterization of the sedimentation test components from the Chinchan Dam

	%wt		kg $CaCO_3$/t			
	%S	%CaCO3	AP	NP	NNP	NP/AP
Underflow	8.75	3.83	273.44	38.25	– 235.19	0.14
Fines	5.96	7.6	186.25	76	– 110.25	0.41
Conc. FeS_2	24.07	0.65	752.19	6.5	– 745.69	0.01
Neutral tailings	1.58	4.93	49.37	49.25	– 0.12	1

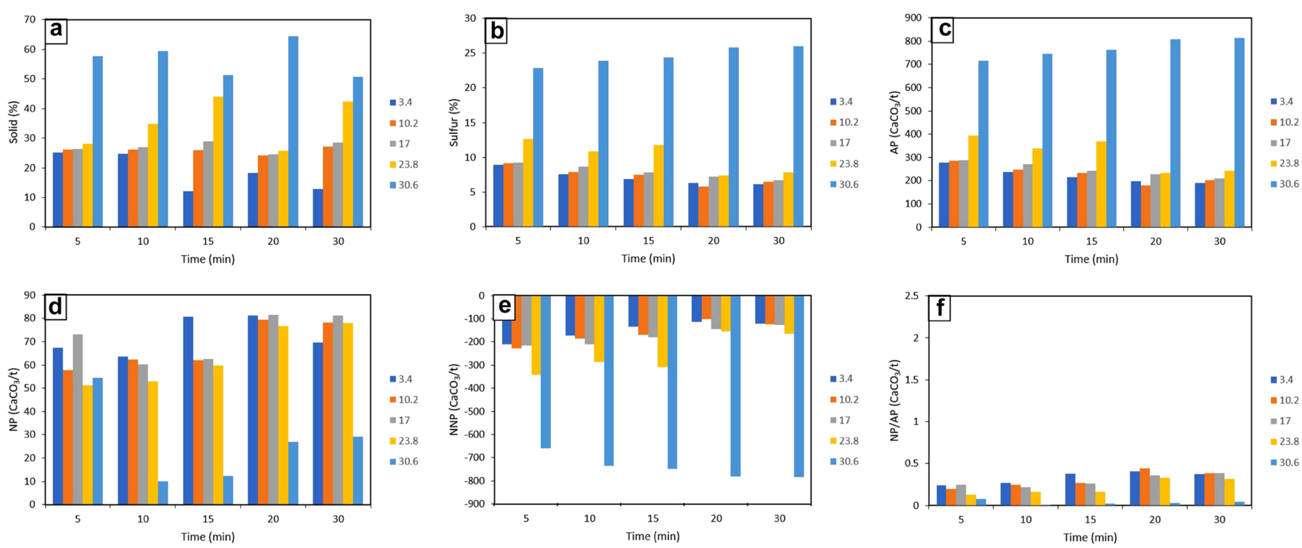

Fig. 6 Variation by layer 1, 2, 3, 4 and 5 (3.4, 10.2, 17, 23.8 and 30.6 cm, respectively) for **a** % solids, **b** % sulfur, **c** AP, **d** NP, **e** NNP, **f** NP/AP as a function of time

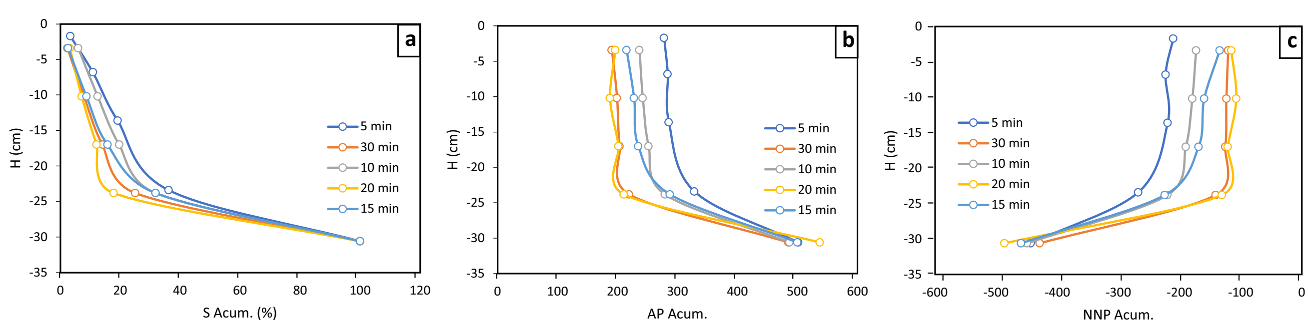

Fig. 7 Variation **a** % sulfur, **b** AP and **c** NNP versus depth as a function of sedimentation time

occurs with the accumulated $CaCO_3$ (Fig. 7b). More than 80% of the sulfur was in the two lower layers, and this percentage increased over time. However, the distribution of $CaCO_3$ is irregular, although it tends to increase in the upper layers and decrease in the lower layer with time; more than 60% of the carbonate is present in the three upper layers. Accordingly, the accumulated AP (Fig. 7c) increased with depth, and the cumulative NP was higher in the upper layers. Logically, the cumulative NNP (Fig. 7c) was moderately negative in the four upper layers, while in the bottommost layer, it was very negative. The cumulative NNP values became less negative with time; this is due to increased sulfur concentration at greater depths being favored, along with sedimentation time.

By separating the pyrite from the tailings by flotation during the final years of operation of a plant, two fundamental aspects could be achieved: (1) a neutral tailings can be produced and used as a cover material for the dam containment wall, and (2) encapsulation of the pyrite concentrate with 2–3 m of fine material with little capacity to generate AMD enhances the chemical stability of the tailings dam and reduces the risk of future AMD.

Since pyrite oxidation is an exothermic reaction, temperature-monitoring probes can be used to evaluate the development of layer performance.

Finally, a brief comparative analysis with traditional tailings management processes implies that the proposed process offers greater chemical stability because the materials with greater capacity for generating acid (pyritic tailings) will be conveniently isolated under water. The encapsulated dam may be covered by organic material and vegetation (Mongil-Manso et al. 2019), consequently requiring less borrowed material, benefitting the surrounding natural environment and would result in lower operating costs in the closing stage. Furthermore, oxygen levels in the fines area is mostly superficial, and is negligible at a depth greater than 2 m (Romero et al. 2007). Unless a tailings dam accident occurs, water infiltration will be prevented by surface structures that capture and divert rain water; other flow is discharged under the dam.

Anticipated lower monitoring and maintenance costs in the post-closure stage are associated with less acid generation over time and, consequently, less contamination of hydrographic basins with acidic waters and dissolved metals. The investment needed to install the proposed tailings management method is much less than the current encapsulation costs, so the centerline construction method is suggested; it is important to note that in this construction method, the dykes are raised vertically on the crest of the existing dam and the downstream slope.

Conclusions

Flotation separation of the pyrite from these tailings will make it possible to produce a neutral tailings that could be used as a cover material for the tailings dam, while the pyrite concentrate could be encapsulated within fine material (slimes) with negligible acid-generating capacity. This method will provide superior chemical stability of the tailings dam since the materials with greater capacity for acid-generation will be conveniently isolated from the environment.

Acknowledgements The authors thank Consulcont S.A.C. for their interest and access to their facilities and Dr. G. T. Lapidus (Universidad Autónoma Metropolitana-Iztapalapa, México) for review and enrichment of this article.

References

ASTM D4513-11 (2017) Standard test method for particle size distribution of catalytic materials by sieving. ASTM International, West Conshohocken. http://www.astm.org

Calla-Choque D (2012) Tratamiento de los residuos del proceso Jarosita de la industria metalúrgica del zinc, con la finalidad de mitigar este pasivo ambiental. MC Thesis, National Univ of Engineering-Lima, Perú

Clesceri LS, Greenberg AE, Eaton AD (1999) Standard methods for the examination of water and wastewater. 20th edition, American Public Health Assoc, American Water Works Assoc, Water Environment Federation

Fairgray ME, Webster-Brown JG, Pope J (2019) Testing geochemical predictions of trace element toxicity and bioavailability at a rehabilitated mine site. Mine Water Environ. https://doi.org/10.1007/s10230-019-00644-y

Gabarrón M, Zornoza R, Acosta JA, Faz Á, Martínez-Martínez S (2019) Mining environments. In: Pereira P (ed) Ch 5, Advances in chemical pollution, environmental management and protection, vol 4. Elsevier, Oxford, pp 157–205

Kottek M, Grieser J, Beck C, Rudolf B, Rubel F (2006) World map of the Köppen-Geiger climate classification updated. Meteorol Z 15(3):259–263. https://doi.org/10.1127/0941-2948/2006/0130

Lottermoser BG (2010) Sulfidic mine wastes. In: Mine wastes. Springer, Berlin. https://doi.org/10.1007/978-3-642-12419-8_2

Mazzeo D, Matera N, De Luca P, Baglivo C, Maria Congedo P, Oliveti G (2020) Worldwide geographical mapping and optimization of stand-alone and grid-connected hybrid renewable system techno-economic performance across Köppen–Geiger climates. Appl Energy 276:115507.

Mongil-Manso J, Díaz-Gutiérrez V, Navarro-Hevia J, Espina M, San Segundo L (2019) The role of check dams in retaining organic carbon and nutrients. A study case in the Sierra de Ávila mountain range (Central Spain). Sci Total Environ 657:1030–1040. https://doi.org/10.1016/j.scitotenv.2018.12.087

Moslemi H, Gharabaghi M (2017) A review on electrochemical behavior of pyrite in the froth flotation process. J Ind Eng Chem 47:1–18. https://doi.org/10.1016/j.jiec.2016.12.012

Olías M, Nieto JM, Pérez-López R, Cánovas CR, Macías F, Sarmiento AM, Galván L (2016) Controls on acid mine water composition from the Iberian Pyrite Belt (SW Spain). CATENA 137:12–23. https://doi.org/10.1016/j.catena.2015.08.018

Romero FM, Armienta MA, González-Hernández G (2007) Solid-phase control on the mobility of potentially toxic elements in an abandoned lead/zinc mine tailings impoundment, Taxco, Mexico. Appl Geochem 22(1):109–127. https://doi.org/10.1016/j.apgeochem.2006.07.017

Santander M, Valderrama L (2019) Recovery of pyrite from copper tailings by flotation. J Mater Res Tech 8(5):4312–4317. https://doi.org/10.1016/j.jmrt.2019.07.041

Santos Jallath JE, Romero FM, Iturbe Argüelles R, Cervantes Macedo A, Goslinga Arenas J (2018) Acid drainage neutralization and trace metals removal by a two-step system with carbonated rocks, Estado de Mexico, Mexico. Environ Earth Sci 77(3):86. https://doi.org/10.1007/s12665-018-7248-2

Vergouw JM, Difeo A, Xu Z, Finch JA (1998) An agglomeration study of sulphide minerals using zeta-potential and settling rate. Part 1: pyrite and galena. Miner Eng 11(2):159–169. https://doi.org/10.1016/s0892-6875(97)00148-9

Wang X-H, Forssberg KSE (1991) Mechanisms of pyrite flotation with xanthates. Int J Miner Process 33(1):275–290. https://doi.org/10.1016/0301-7516(91)90058-Q

Wang L, Ji B, Hu Y, Liu R, Sun W (2017) A review on in situ phytoremediation of mine tailings. Chemosphere 184:594–600. https://doi.org/10.1016/j.chemosphere.2017.06.025

Younger PL, Banwart SA, Hedin RS (2002) Mine water hydrology, pollution, remediation. Kluwer Academic Publishers, Dordrecht